J Mater Sci (2007) 42:7843–7849
DOI 10.1007/s10853-007-1629-3

Characterization of macroporous carbonate-substituted hydroxyapatite bodies prepared in different phosphate solutions

Yoong Lee · Yeong Min Hahm · Shigeki Matsuya · Masaharu Nakagawa · Kunio Ishikawa

Received: 31 July 2006 / Accepted: 20 February 2007 / Published online: 1 June 2007

Abstract Bone mineral of human is different in composition from the stoichiometric hydroxyapatite ($Ca_{10}(PO_4)_6(OH)_2$) in that it contains additional ions, of which CO_3^{2-} is the most abundant species. Carbonate-substituted hydroxyapatite (CHA) bodies were prepared by the hydrothermal treatment of highly porous calcium carbonate ($CaCO_3$) body at 120 °C in 1 M M_2HPO_4 and M_3PO_4 solutions (M = NH_4 or K). It was found that $CaCO_3$ body was almost transformed into CHA body after hydrothermal treatment for 24 h irrespective of type of phosphate solution. However, a small amount of $CaCO_3$ still remained after the treatment in K_3PO_4 for 48 h. Crystal shape of CHA bodies prepared in those solutions except for K_2HPO_4 was flake-like, which was different from that (stick-like) of original $CaCO_3$ body used for the preparation of CHA body. CHA prepared in the K_2HPO_4 showed globule-like crystal. Average pore size and hole size of the CHA bodies were 150, 70 μm and their porosities were about 89% irrespective of the solution. Carbonate content was slightly higher in the CHA bodies obtained from potassium phosphate solutions than in those obtained from ammonium phosphate solutions. Mostly B-type CHA was obtained after the hydrothermal treatment in the potassium phosphate solutions. On the other hand, mixed A- and B-type CHA (ca. 1–2 in molar ratio) was obtained in the ammonium phosphate solutions. The content of CO_3^{2-} in the CHA body depended on the type of phosphate solution and was slightly larger in the potassium phosphate solutions.

Y. Lee (✉) · S. Matsuya · M. Nakagawa · K. Ishikawa
Department of Biomaterials, Faculty of Dental Science, Kyushu University, 3-3-1 Maidashi, Higashiku Fukuoka 812-8582, Japan
e-mail: ly02147@gmail.com

Y. Lee · Y. M. Hahm
Department of Chemical Engineering, College of Engineering, Dankook University, Seoul 140-714, Korea

Introduction

The mineral phase of human hard tissue consists of hydroxyapatite (HA: $Ca_{10}(PO_4)_6(OH)_2$) containing a variety of impurity ions such as carbonate, sodium, and magnesium etc. [1–5]. Carbonate is one of the most abundant impurity ions and its content is about 4–8 wt% [6–8]. In this sense, hard tissue is regarded as carbonate-substituted HA (CHA). It has been reported that synthetic CHA revealed the biological activity better than synthetic HA because the incorporation of carbonate into HA caused an increase in solubility, a decrease in crystallinity, a change in crystal morphology, and an enhancement of chemical reactivity owing to the weak bonding [2, 9, 10]. CHA is actually more soluble in vivo than HA and increases the local concentration of calcium and phosphate ions that are necessary for new bone formation [11–13]. For these reasons, the recent researches have focused on CHA in comparison with HA. Carbonate ion in CHA can be present at two different sites in the apatite lattice [14–18]. One is in hydroxyl site (channel site), called A-type CHA (A-CHA), and the other is in phosphate site, called B-type CHA (B-CHA). These two carbonate types can be distinguished by their infrared spectra: A-type carbonate shows a doublet band at about 1,545 and 1,450 cm^{-1} (asymmetric stretching vibration) and a singlet band at 880 cm^{-1} (out-of-plane bending vibration) and B-type shows the corresponding bands at about 1,455 and 1,410, and 875 cm^{-1},

respectively. A-CHA and B-CHA are abundant in bone of the old and the young, respectively [19]. A-CHA is generally prepared by heating HA at high temperature (800–1,000 °C) under dry carbon dioxide atmosphere as a source of carbonate [19, 20]. In case of B-CHA, it is synthesized by precipitation method and hydrothermal treatment, employing various starting materials. It has been reported that human trabecular osteoclastic cells have low affinity towards A-CHA surface compared to HA [10, 21], whereas B-type substitution can enhance the solubility without changing the surface energy of CHA that affects the initial cell attachment and the collagenous matrix deposition [22, 23]. Even though many researches have been carried out concerning the preparation of CHA, they were related to CHA in the form of powder [7, 9, 16, 19, 20].

In the present study, macroporous CHA bodies were prepared through hydrothermal treatment of porous calcite monolith in various phosphate solutions. The CHA bodies were characterized in terms of chemical and physical properties, such as extent of transformation of $CaCO_3$ body into CHA body, type and content of carbonate and crystal morphology.

Materials and methods

Preparation of CHA body

Calcium hydroxide ($Ca(OH)_2$; Wako Chemicals, Japan) and sodium chloride(NaCl; Wako Chemicals, Japan) were used for the preparation of macroporous $CaCO_3$ body. Ground and sieved NaCl with particle size of 106–300 μm was added to $Ca(OH)_2$ to make a mixture of $Ca(OH)_2$ and 85.7 wt% NaCl. The mixture was put in a stainless steel mold (10 mm in inner diameter) and pressed uniaxially at 10 MPa to prepare $Ca(OH)_2$/NaCl composite. The composite was carbonated in carbon dioxide reaction vessel for 90 h at room temperature. Subsequently, it was washed with distilled water at 90 °C over 3 days to drive off soluble components including NaCl and dried at 60 °C for 24 h. The macroporous $CaCO_3$ body was then treated hydrothermally in 1 M phosphate solutions at 120 °C for various times. Phosphates used are diammonium hydrogen phosphate ($(NH_4)_2HPO_4$; Wako Chemicals, Japan), triammonium phosphate ($(NH_4)_3PO_4 \cdot 3\ H_2O$; Wako Chemicals, Japan), dipotassium hydrogen phosphate (K_2HPO_4; Wako Chemicals, Japan) and tripotassium phosphate (K_3PO_4; Wako Chemicals, Japan). The overall Ca/P molar ratio was 5/9 in which P is three times more than that needed for a stoichiometric HAP formation. Each body after the hydrothermal treatment was washed with distilled water for 6 h to eliminate soluble ions.

Characterization

X-ray diffraction (XRD) analysis

Purity and crystallite size of the CHA formed were determined by XRD (RINT 2500V, Rigaku, Japan) analysis. The XRD pattern was obtained in the range of 2θ from 10 to 60 ° in a continuous mode at a scanning rate of 2 °/min.

Scanning electron microscope (SEM) analysis

Morphology of fracture surface and crystal shape were observed by SEM (JSM 5400LV, JEOL, Japan). Average crystal thickness, average NaCl-print size that can be attributed to the pore size and hole size formed in pore were analyzed by means of image analysis software(USB Digital Scale V1.0, Scalar Corporation).

Fourier Transform Infrared (FT-IR) spectroscopy

Infrared spectra between 400 and 4,000 cm^{-1} were recorded on FT-IR spectrometer (Spectrum 2000, Perkin–Elmer, USA) to examine structural changes by the hydrothermal treatment, in particular, CO_3^{2-} ions substituting for PO_4^{3-} and/or OH^- ions.

Mechanical strength analysis

Compressive strength of the CHA body was evaluated at a constant crosshead speed of 1 mm/min on an universal testing machine (SV-301, IMADA, Japan). Five samples were tested for each experimental condition.

Chemical analysis

Carbon and nitrogen content were determined using CHN elemental analyzer (CHN coder-MT-6, Yanaco, Japan). Calcium and potassium, and phosphorus content were determined by an atomic absorption spectrometer (AAnalyst 300, Perkin–Elmer, Japan) and a spectrophotometer (Ubest-50, Jasco, Japan), respectively.

Porosity measurement

Apparent density was calculated from their weight and dimensions. Relative density was calculated by the ratio of the apparent density to the true density. True density of the $CaCO_3$ body treated hydrothermally for 24 h was measured using a picnometer. The total porosity of the body is defined as follows;

Total porosity(%) = 100(%)–relative density(%)

The total porosity was obtained as the average value of five bodies.

Results and discussion

Figure 1 shows XRD patterns of $CaCO_3$ body after the hydrothermal treatment in the phosphate solutions for various times. Hydroxyapatite (HA) phase was detected as a main reaction product regardless of time and type of phosphate solution. Transformation of $CaCO_3$ into HA in ammonium phosphate solution (c and d) seemed to proceed faster than that in potassium phosphate solution (a and b). With the hydrothermal treatment in ammonium phosphate solutions, transformation of $CaCO_3$ into HA was almost completed even after 6 h. With the potassium phosphate solutions, $CaCO_3$ (peak shown by an arrow) still remained after 6 h. Transformation into HA completed after 24 h in K_2HPO_4, however, a small amount of β-TCP (shown by * in Fig. 1a) was also formed as by-product. On the other hand, though β-TCP was not formed in K_3PO_4 solution, $CaCO_3$ remained even after 48 h, as shown in Fig. 1b. This is probably due to high pH in K_3PO_4 solution, which resulted in stabilization of $CaCO_3$ comparing with carbonate apatite. Actually, solubility difference between both compounds decreased with increasing in pH and almost comparable above pH of 9 [24]. XRD patterns of HA showed a different feature in an extent of separation between (211) and (112) diffraction peaks around 2θ of 32 °. In both of the phosphate solutions, the peaks were well separated in the secondary phosphate solutions comparing with the tertiary phosphate solutions. Those two peaks were almost merged in K_3PO_4 solution. Such a change is often observed when the lattice parameter of a-axis in a hexagonal apatite crystal decreased with increasing in CO_3 content [25]. Table 1 shows the lattice parameter of the apatite phase after the hydrothermal treatment in the phosphate solutions for 24 h calculated from a least square method using the

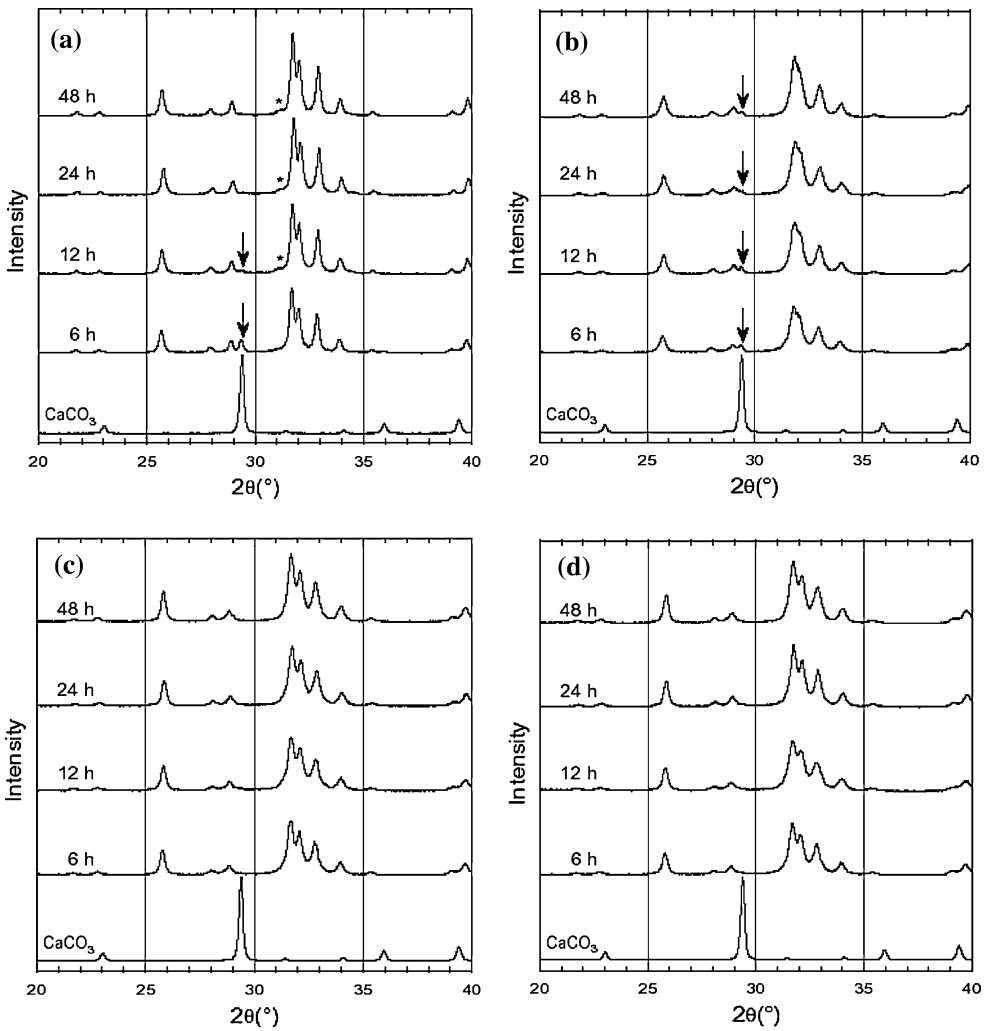

Fig. 1 Change in XRD patterns of CHA bodies hydrothermally treated in various phosphate solutions with time. (**a**) K_2HPO_4, (**b**) K_3PO_4, (**c**) $(NH_4)_2HPO_4$, (**d**) $(NH_4)_3PO_4$

Table 1 Lattice parameters and crystallite size of HA formed after the hydrothermal treatment in various phosphate solutions at 120 °C for 24 h

Solution	Lattice parameter (Å)		Crystallite size (Å)
	a-axis	*c*-axis	
$(NH_4)_2HPO_4$	9.427(0.008)	6.887(0.004)	312
$(NH_4)_3PO_4$	9.439(0.007)	6.894(0.003)	311
K_2HPO_4	9.422(0.008)	6.922(0.004)	601
K_3PO_4	9.386(0.006)	6.904(0.003)	241

diffraction peaks between 10 and 60°. HA formed in K_3PO_4 solution actually showed the smallest *a*-axis parameter among all. It was reported that pure hydroxyapatite showed *a*-axis of 9.421 Å and *c*-axis of 6.88 Å [26]. CHA obtained in the secondary phosphate solutions had almost the same *a*-axis value as the pure hydroxyapatite. However, the CHA obtained in $(NH_4)_3PO_4$ had a larger *a*-axis and that in K_3PO_4 had a smaller one. It is reported that there are two types of CHA, in which PO_4^{3-} lattice site is substituted by CO_3^{2-} (B-type) and OH^- lattice site is substituted by CO_3^{2-} (A-type) [27]. With increasing in CO_3 content of carbonate apatite, *a*-axis increased in A-type CHA and decreased in B-type CHA [28]. The change in *a*-axis described above is closely related to the formation of both type of CHA as discussed later. Crystallinity of HA prepared in K_2HPO_4 solution seems to be the highest, judging from the half width of peaks. Table 1 also shows crystallite sizes of the apatite phase calculated from the half width of the diffraction peaks based on Scherrer's formula [29]. With the ammonium phosphate solution, crystallite sizes of HA were almost the same in both of the slats ($(NH_4)_2HPO_4$: 312 Å, $(NH_4)_3PO_4$: 311 Å). With the potassium solutions, however, crystallite size was much smaller in K_3PO_4 (241 Å) than in K_2HPO_4 (601 Å).

Figure 2 shows FT-IR spectra after the hydrothermal treatment of $CaCO_3$ for 24 h in the phosphate solutions. The typical CO_3^{2-} bands were observed at 1,550–1,400 (ν_3) and 880–870 cm^{-1} (ν_2), and PO_4^{3-} bands at 980–1,100 (ν_3), 960(ν_1) and 560–600 cm^{-1}(ν_4), respectively. There were no peaks of hydrogen phosphate (HPO_4^{2-}, 906, 852 and 530 cm^{-1}) irrespective of types of phosphate solutions [9, 30, 31]. Existence of CO_3^{2-} band in those spectra clearly shows CO_3^{2-}-substituted HA (CHA) formation. B-type CHA shows CO_3 band at about 1,410 and 1,455 cm^{-1}, and A-type at about 1,545 and 1,455 cm^{-1} [32]. With the ammonium phosphate solutions, the CO_3^{2-} band appeared at 1,545, 1,455 and 1,410 cm^{-1}. This observation showed the CHA formed in the ammonium phosphate solutions contained both A-type and B-type CO_3^{2-}. On the other hand, with the potassium phosphate solutions, the band appeared at 1,455 and 1,410 cm^{-1}, which indicates B-type CHA formation. Landi et al. [19] reported that a weight ratio of A- and B-type CO_3^{2-} could be estimated from the intensity ratio of two peaks at 880 and 873 cm^{-1} in the IR spectrum. As shown in Fig. 2b, ν_2CO_3 band was

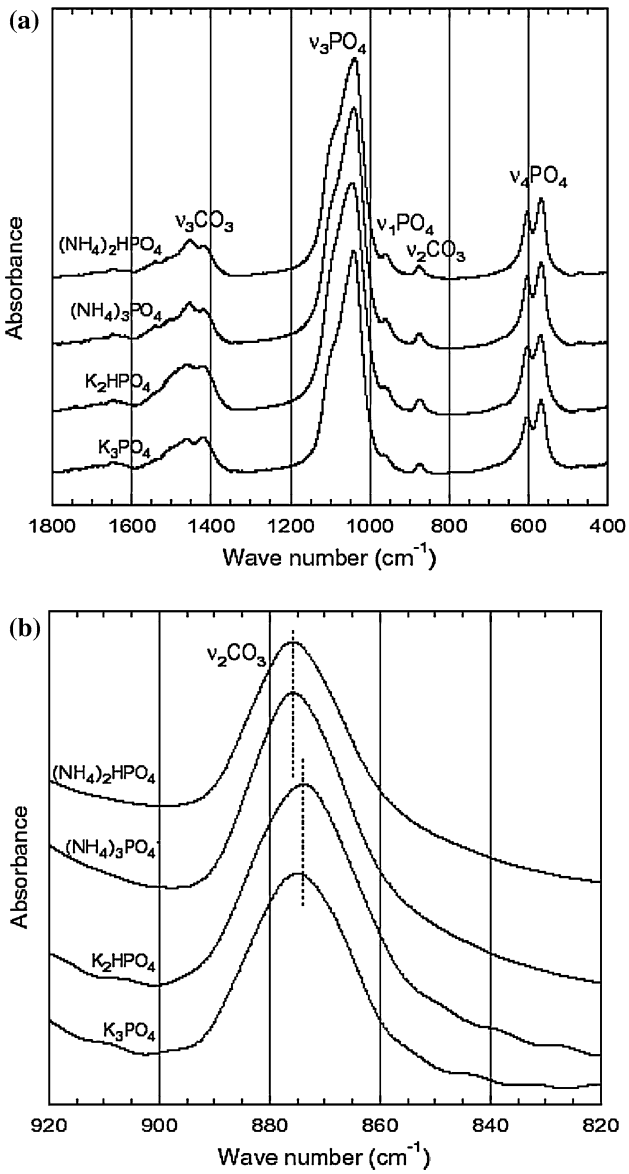

Fig. 2 FT-IR spectra of CHA bodies prepared hydrothermally in various phosphate solutions for 24 h (**a**) and its expanded ν_2CO_3 region (**b**)

observed at slightly higher wave number for the CHA obtained in ammonium phosphate solutions than for that in potassium phosphate solutions. However, the two peaks appeared about 876 and 874 cm^{-1}, which were between the wave number for A-type and B-type CHA. This fact suggests that the peaks consisted of overlapped one of A- and B-type CHA. Therefore we tried to separate the peak graphically using a computer software(Peak Fit, SPSS Inc, Chicago IL, USA). The analysis showed that A/B-type weight ratios were 0.53($(NH_4)_2HPO_4$), 0.54($(NH_4)_3PO_4$), 0.01(*hbox*K_2HPO_4) and 0 (*hbox*K_3PO_4). The result suggests that mixed type CHA (A/B-CHA) was formed in the ammonium phosphate solutions and mostly B-type CHA (B-CHA) was formed in the potassium phosphate solutions. It has been reported that an increase in A-type CO_3^{2-} content in A/B-CHA by means of the migration of B-type CO_3^{2-} to OH^- lattice site with heat treatment caused a decrease in crystallinity, which was attributed to the fact that the hydroxyl site can accept more vacancies and the CO_3^{2-} ion has consequently more degree of freedom that cause the increase in disorder [19]. However, in this study, the crystallinity of A/B-CHA obtained in the ammonium phosphate solutions was high compared with that of B-CHA obtained in the potassium phosphate solutions, as shown in Fig. 1.

Table 2 summarizes chemical composition of the CHA obtained by the hydrothermal analysis for 24 h in various phosphate solutions. OH content was calculated from Eq. (1) on the basis of the electroneutrality condition [4].

$$\frac{\text{wt\% OH}}{M_{\text{OH}}} = 2\frac{\text{wt\% Ca}}{M_{\text{Ca}}} + \frac{\text{wt\% K[or NH}_4\text{]}}{M_{\text{K[orNH}_4\text{]}}} - 3\frac{\text{wt\% PO}_4}{M_{\text{PO}_4}} - 2\frac{\text{wt\% CO}_3}{M_{\text{CO}_3}} \quad (1)$$

M_X in Eq. (1) is the atomic or ionic mass of X. As shown in Table 2, Ca/P ratio showed almost the same value of 1.72–1.73 for the solutions except for K_3PO_4 solution, which had a slightly larger value of 1.84. The CO_3^{2-} content was slightly larger in the potassium phosphate solutions than in the ammonium phosphate solutions. K^+ion was incorporated into CHA more easily than NH_4^+. The main reason for this result can be attributed to the difference in ionic radius between K^+(1.38Å) and NH_4^+ (1.43 Å), meaning that K^+ ions can be more easily replaced with Ca^{2+} (1.00 Å) ions in order to compensate for extra negative charge caused by the substitution of CO_3^{2-} for PO_4^{3-} ions. Chemical formula was obtained based on the chemical composition in Table 2 and A/B CO_3^{2-} ratio from FT-IR analysis and is shown in Eqs. (2)–(5).

$$K_2HPO_4 : Ca_{8.18}K_{0.5}(PO_4)_{4.72}(CO_3)_{1.28}(OH)_{0.1}(CO_3)_{0.02} \quad (2)$$

$$K_3PO_4 : Ca_{8.82}K_{0.42}(PO_4)_{4.79}(CO_3)_{1.21}(OH)_{1.27} \quad (3)$$

$$(NH_4)_2HPO_4 : Ca_{9.23}(NH_4)_{0.12}(PO_4)_{5.36}(CO_3)_{0.64}(OH)_{0.54}(CO_3)_{0.34} \quad (4)$$

$$(NH_4)_3PO_4 : Ca_{9.21}(NH_4)_{0.19}(PO_4)_{5.34}(CO_3)_{0.66}(OH)_{0.18}(CO_3)_{0.36} \quad (5)$$

In the above calculation, it was assumed that PO_4 site has no vacancy, that is, th e total number of subscript ofPO_4^{3-} and CO_3^{2-} ions should be 6. Six types of basic substitution mechanisms have been proposed in literatures [4, 15]. Among these, $Ca^{2+} + PO_4^{3-} + OH^- \Leftrightarrow V_{Ca}$ $CO_3^{2-} + V_{OH}$[mechanism I] and$Ca^{2+} + PO_4^{3-} \Leftrightarrow M^+ + CO_3^{2-}$ [mechanism III] for B-type carbonate substitution was reported as main mechanisms [4]. The chemical formula for B-CHA based on these two mechanisms can be described as follows:

$$Ca_{10-x-y}M_y(PO_4)_{6-x-y}(CO_3)_{x+y}(OH)_{2-x}, \quad (6)$$

where x and y represent the contribution of mechanism I and III, respectively and M stands for alkali or ammonium ion. Main mechanism of A-type carbonate substitution was also proposed as $2OH^- \Leftrightarrow V_{OH} + CO_3^{2-}$ [mechanism V] [19]. If both A- and B-type carbonate substitutions take place simultaneously, the chemical formula for A/B-CHA should be expressed as Eq. (7).

$$Ca_{10-x-y}M_y(PO_4)_{6-x-y}(CO_3)_{x+y}(OH)_{2-x-2z}(CO_3)_z, \quad (7)$$

where z represents the contribution of mechanism V. If x, y and z are calculated using Eq. (6) or (7) from subscript for

Table 2 Chemical composition of CHA prepared by the hydrothermal treatment in various phosphate solutions for 24 h

Phosphate	Ca [wt%]	P [wt%]	Ca/P Molar ratio	NH_4 [wt%]	K [wt%]	CO_3 [wt%]	OH [wt%]
$(NH_4)_2HPO_4$	38.22	17.16	1.72	0.22	–	6.05	0.95
$(NH_4)_3PO_4$	38.18	17.13	1.72	0.34	–	6.3	0.33
K_2HPO_4	34.74	15.5	1.73	–	2.06	8.24	0.18
K_3PO_4	35.86	15.04	1.84	–	1.67	7.39	2.19

CO_3 and K in Eqs. (2) or (3), the values are 0.78(x), 0.5(y) and 0.02(z) for Eq. (2) and 0.79(x) and 0.42(y) for Eq. (3), respectively. These values gave 8.72 and 1.18 for the subscripts for Ca and OH in Eq. (7), and 8.79 and 1.21 for those in Eq. (8), respectively. The latter subscripts well agreed with those in Eq. (3), however the former did not. This fact suggests that other mechanism also should be taken into account to explain the substitution in the CHA obtained in the K_2HPO_4 solution, besides the above mechanisms. On the other hand, with CHA obtained in the ammonium phosphate solutions, the subscripts for Ca and OH are 9.36 and 0.8 for Eq. (4), and 9.34 and 0.81 for Eq. (5), respectively, when they are calculated in the same way as above. In this case, the former values agreed satisfactorily with the corresponding subscripts in Eq. (4) for CHA obtained in the $(NH_4)_2HPO_4$ solution. The latter values, however, did not agree well, indicating that the other substitution mechanism also should be taken into account again.

Figure 3 shows SEM photographs of CHA obtained in the various phosphate solutions. Crystal shapes of the CHA are quite different from that of the original $CaCO_3$ and largely depend on the type of phosphate solution, as shown in Fig. 3. Most of the CHA crystal showed a flake-like morphology except for the CHA formed in K_2HPO_4. However, crystallite size was much smaller in the CHA obtained in the tertiary phosphate solutions. On the other hand, fine globule-like crystals were formed in the CHA formed in K_2HPO_4 solution (Fig. 3c). A typical fracture surface of the CHA prepared in K_2HPO_4 solution is shown in Fig. 3b.

Those of the CHA prepared in the other solutions also showed a similar structure. Macropores and the holes connecting those pores are seen in the fracture surface. Average pore and hole size were about 150 μm and 70 μm, respectively, irrespective of the type of solutions. Porosity calculated from the relative density was 88–89% in all of the CHA except for the CHA obtained in the K_3PO_4 solution, which was broken into a few pieces during the hydrothermal treatment and didn't keep its original shape. Compressive strength of the CHA was 123 kPa ($(NH_4)_2HPO_4$), 81 kPa ($(NH_4)_3PO_4$) and 64 kPa (K_2HPO_4), which is harder than that (53 kPa) of the original $CaCO_3$ body. The difference in compressive strength

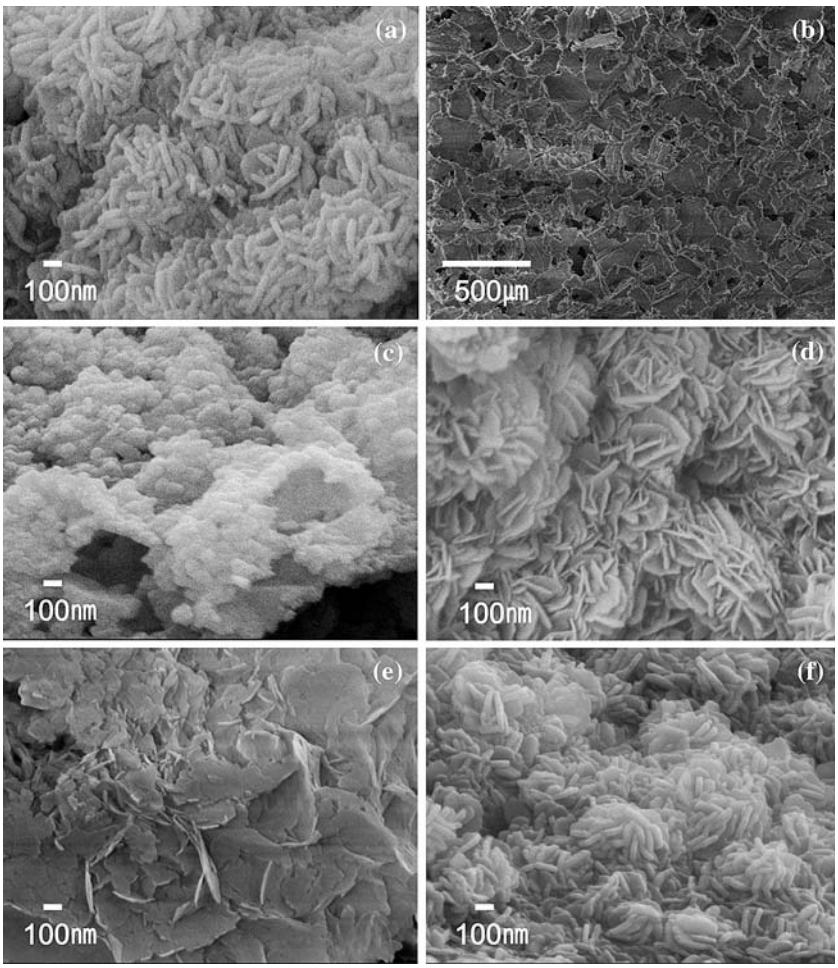

Fig. 3 Scanning electron microscopic observation of $CaCO_3$ and CHA bodies prepared hydrothermally in the various phosphate solutions for 24 h. (**a**) crystal shape of $CaCO_3$ (**b**) fracture surface of CHA prepared in K_2HPO_4 (**c**) crystal shape of CHA prepared in K_2HPO_4 (**d**) crystal shape of CHA prepared in K_3PO_4 (**e**) crystal shape of CHA prepared in $(NH_4)_2HPO_4$ (**f**) crystal shape of CHA prepared in $(NH_4)_3HPO_4$

for the CHA is presumably related to the difference in crystallite size and crystal shape because other properties, such as porosity and average pore and hole size, are similar each other.

Conclusions

CHA, carbonate-substituted hydroxyapatite, bodies were prepared by the hydrothermal treatment of pure $CaCO_3$ body at 120 °C in secondary and tertiary ammonium or potassium phosphate solutions. Transformation of $CaCO_3$ into CHA was almost completed by the hydrothermal treatment for 24 h except for K_3PO_4 solution, in which a small amount of $CaCO_3$ remained even after 48 h. Carbonate content of the CHA was slightly higher with potassium phosphate solutions than with ammonium phosphate solutions. Mostly B-type CO_3^{2-} substitution takes place when $CaCO_3$ body is treated hydrothermally in the potassium phosphate solutions. On the other hand, mixed A- and B-type CHA was obtained in the ammonium phosphate solutions. The content of CO_3^{2-} in the CHA body depended on the type of phosphate solution. The average pore and hole size were about 150 and 70 μmin all of the solutions.

Acknowledgements This study was supported in part by a Grant-in-aid for Scientific Research from the Ministry of Education, Sports, Culture, Science, and Technology, Japan

References

1. Rau JV, Cesaro SN, Ferro D, Barinov SM, Fadeeva JV (2004) J Biomed Mater Res Part B: Appl Biomater 71B(2):441
2. Baig AA, Fox JL, Su J, Wang Z, Otsuka M, Higuchi WI, Legeros RZ (1996) J Colloid Interface Sci 179:608
3. Tang R, Henneman ZJ, Nancollas GH (2003) J Cryst Growth 249:614
4. Rieters IY, Maeyer EAPD, Verbeeck RMH (1996) Inorg Chem 35:5791
5. Wenk HR, Heidelbach F (1999) Bone 24(4):361
6. Landi E, Tampieri A, Celotti G, Langenati R, Sandri M, Sprio S (2005) Biomaterials 26:2835
7. Barralet J, Best S, Bonfield W (1998) J Biomed Mater Res 41(1):79
8. Barralet J, Akao M, Aoki H (2000) J Biomed Mater Res 49(2):176
9. Suchanek WL, Shuk P, Byrappa K, Riman RE, Tenhuisen KS, Janas VF (2002) Biomaterials 23:699
10. Redey SA, Nardin M, Assolant DB, Rey C, Delannoy P, Sedel L, Marie PJ (2000) J Biomed Mater Res 50(3):353
11. Barralet JE, Aldred S, Wright AJ, Coombes AGA (2002) J Biomed Mater Res 60:360
12. Matsumoto T, Okazaki M, Inoue M, Ode S, Chien CC, Nakao H, Hamada Y, Takahashi J (2002) J Biomed Mater Res 60:651
13. Barralet JE, Best SM, Bonfield W (2000) J Mater Sci: Mater Med 11:719
14. Tonsuaadu K, Peld M, Leskela T, Mannonen R, Niinisto L, Veiderma M (1995) Thermochim Acta 256:55
15. Feki HE, Savariault JM, Salah AB, Jemal M (2000) Solid State Sci 2:577
16. Oliverira LM, Rossi AM, Lopes RT (2000) Appl Radiat Isotopes 52:1093
17. Fleet ME, Liu X (2004) J Solid State Chem 177:3174
18. Fleet ME, Liu X, King PL (2004) Am Mineral 89:1422
19. Landi E, Tampieri A, G Celotti, Vichi L, Sandri M (2004) Biomaterials 25:1763
20. Fleet ME, Liu X (2003) J Solid State Chem 174:412
21. Redey SA, Razzouk S, Rey C, Assollant DB, Leroy G, Nardin M, Cournot G (1999) J Biomed Mater Res 45:140
22. Ellies LG, Lelson DGA, Featherstone JDB (1988) J Biomed Mater Res 22:541
23. Navarro M, Valle SD, Martinez S, Zeppetelli S, Ambrosio L, Planell JA, Ginebra MP (2004) Biomaterials 25:4233
24. Verveecke G, Lemaitre J (1990) J Cryst Growth 104:820
25. Legeros RZ, Trautz OR (1967) Science 155:1409
26. Legeros RZ (1991) In: Meyers HM (ed) Monographs in oral science, vol 15. KARGER, Basel, p 18
27. Bonel G, Montel G (1964) Comp Rend Acad Sci (Paris) 258:923
28. Legeros RZ (1991) In: Meyers HM (ed) Monographs in oral science, vol 15. KARGER, Basel, p 89
29. Cullity BD (1978) Elements of X-ray Diffraction, 2nd edn. Addison-Wesley Pub Co Inc, Philippines, p 102
30. Bouhaouss A, Bensaoud A, Laghzizil A, Ferhat M (2001) Int J Inorg Mater 3:437
31. Dekker RJ, Bruijn JDD, Stigter M, Barrere F, Layrolle P, Blitterswijk CAV (2005) Biomaterials 26:5231
32. Elliott JC (1994) Structure and chemistry of the apatites and other calcium orthophosphates. Studies in Inorganic Chemistry 18, Elsevier, Amsterdam, pp 230–234